6-1-2004

Leader-to-Formation Stability

Herbert G. Tanner
University of Pennsylvania

George J. Pappas
University of Pennsylvania, pappasg@seas.upenn.edu

Vijay Kumar
University of Pennsylvania, kumar@grasp.upenn.edu

Suggested Citation:
Tanner, Herbert G., George J. Pappas and Vijay Kumar. (2004). *Leader-to-Formation Stability.* IEEE Transactions on Robotics. Vol. 20(3). p. 443-455.

Leader-to-Formation Stability

Abstract
The paper investigates the stability properties of mobile agent formations which are based on leader-following. We derive nonlinear gain estimates that capture how leader behavior affects the interconnection errors observed in the formation. Leader to formation stability (LFS) gains quantify error ampli£cation, relate interconnection topology to stability and performance and offer safety bounds for different formation topologies. Analysis based on the LFS gains provides insight to error propagation and suggests ways to improve the safety, robustness and performance characteristics of a formation.

Disciplines
Engineering | Mechanical Engineering

Comments
Suggested Citation:
Tanner, Herbert G., George J. Pappas and Vijay Kumar. (2004). *Leader-to-Formation Stability.* IEEE Transactions on Robotics. Vol. 20(3). p. 443-455.

Leader-to-Formation Stability

Herbert G. Tanner George J. Pappas Vijay Kumar

***Abstract*— The paper investigates the stability properties of mobile agent formations which are based on leader-following. We derive nonlinear gain estimates that capture how leader behavior affects the interconnection errors observed in the formation. Leader to formation stability (LFS) gains quantify error ampli£cation, relate interconnection topology to stability and performance and offer safety bounds for different formation topologies. Analysis based on the LFS gains provides insight to error propagation and suggests ways to improve the safety, robustness and performance characteristics of a formation.**

I. Introduction

Interconnected systems have lately received considerable attention, motivated by recent advances in computation and communication, which provide the enabling technology for applications such as automated highway systems [1], cooperative robot reconnaissance [2], [3] and manipulation [4], [5], formation ¤ight control [6], [7], satellite clustering [8] and control of groups of unmanned vehicles [9], [10], [6]. Advantages of interconnected multi-agent systems over conventional systems include reduced cost, increased ef£ciency, performance, recon£gurability and robustness, and new capabilities. A space radar based on satellite clusters [11] is estimated to cost three times less than currently available systems, increase geolocation accuracy by a factor of 500, offer two orders of magnitude smaller propulsion requirement and be able to track moving targets through formation ¤ight.

Formations have been represented by means of virtual structures or templates [12], [7]. Graphs have also been used to capture the interconnection topology in a formation [13], [14] and re¤ect control structure [15], constraint feasibility [16], information ¤ow [17] and error propagation [18]. These graphs can have undirected edges, when the latter model position constraints [13], [14], or directed for the case of information ¤ow [17] or leader-following inter-agent control speci£cations [19], [20], [21].

Formation control and interconnected systems stability have been analyzed recently from many different perspectives. In behavior-based approaches [2] the group behavior emerges as a combination of group member behaviors, selected among a set of primitive actions. Lyapunov based techniques have been used extensively to establish asymptotic stability in multi-agent formations. Formation control speci£cations are usually encoded in a formation constraint function [22] or in some arti£cial potential functions [23], [13] that usually play the role of Lyapunov function candidates. Another approach that applies to linear spatially interconnected systems is a distributed control scheme [24] that is based on $\mathcal{L}_2$-norm performance measures. Local coordination control schemes that aim at stabilizing agents around some desired con£gurations have also been successfully applied [7], [19], [25]. String stability has proved to be an important tool in analyzing the stability of platoons of vehicles [26], [27], [28], [29]. System cascading is made stable by ensuring that the error attenuates as it propagates from one system to the next downstream. The string stability property is given an elegant state space formulation and it was shown to be robust with respect to structural perturbations [1]. Mesh stability, which can be thought of as a generalization to multiple dimensions [30], also enjoys similar properties.

In the new generation of interconnected systems that are now being developed, safety, robustness and performance are going to be critical properties, and distinguish such systems from all their predecessors. Most previous approaches to formation control aim at establishing convergence properties for formation errors, which is necessary to make such a system operational. To address issues related to safety and performance, we need new tools [31] that allow as to quantify, bound and estimate the error amplitudes in the worst case.

In this paper we introduce *Leader-to-Formation Stability (LFS)* in an effort to address these issues. The notion is based on input-to-state stability [32] and its invariance properties under cascading [33], [34]. LFS quanti£es error ampli£cation during signal propagation in leader-following formations. We establish nonlinear gain estimates between the errors of the formation leaders and the interconnection errors observed inside the formation. In this way, we can characterize how leader inputs and disturbances affect the stability of the group. We are also able to assess the stability of particular subgroups inside the formation and thus guide analysis. In the case where the gain estimates can be expressed as linear functions of the formation errors, then gain propagation can be done ef£ciently through an algorithm based on algebraic matrix formulas, in which the interconnection topology of the formation appears explicitly in the form of the adjacency matrix of the underlying graph.

II. Definitions and Preliminary Remarks

In the context of this paper, a formation is de£ned as a network of vehicles interconnected via their controller speci£cations. These speci£cations dictate that each agent must maintain a certain relative state vector with respect to its leaders. Agent interconnections are modeled as edges in a directed (formation) graph [35], labeled by the respective control speci£ca-

Herbert Tanner is with the Department of Electrical and Systems Engineering, 3401 Walnut Street, Suite 301C, University of Pennsylvania, Philadelphia, PA 19104-6228 (e-mail:tanner@grasp.cis.upenn.edu)

George Pappas is with the Department of Electrical and Systems Engineering, 200 South 33rd Street, University of Pennsylvania, Philadelphia, PA 19104 (e-mail:pappasg@ee.upenn.edu)

Vijay Kumar is with the Department of Mechanical Engineering and Applied Mechanics, 3401 Walnut Street, Suite 301C, University of Pennsylvania, Philadelphia, PA 19104-6228, (e-mail:kumar@grasp.cis.upenn.edu)

tions. This section introduces the material needed for describing formally the formation, and de£nes the stability notions that are going to be used in the subsequent analysis.

A. Graph Theory Preliminaries

A *directed graph* consists of a vertex set $V(X)$ and an directed edge set $E(X)$, where a directed edge is an ordered pair of distinct vertices.An edge (x, y) in a directed graph is said to be incoming with respect to y and outcoming with respect to x. Such an edge has vertex x as a *tail* and vertex y as a *head*. The *indegree* of a vertex in a directed graph is de£ned as the number of edges that have this vertex as a head. If (x, y) is an edge, then x and y are *adjacent*. A *subgraph* of a graph X is a graph Y such that $V(Y) \subseteq V(X)$ and $E(Y) \subseteq E(X)$. A subgraph Y of X is an *induced subgraph* when any two adjacent vertices in $V(Y)$ are also adjacent in X. A *path* of length r in a directed graph is a sequence $v_0, \ldots, v_r$ of distinct vertices such that for every $i \in [1, r]$, $(v_i, v_{i+1}) \in E$. A *weak path* is a sequence $v_0, \ldots, v_r$ of $r+1$ distinct vertices such that for each $i \in [1, r]$ either (v_i, v_{i+1}) or (v_{i+1}, v_i) is an edge in E. A directed graph is *weakly connected* or simply *connected* if any two vertices can be joined with a weak path. The *distance* between two vertices x and y in a graph X is the length of the shortest path from x to y. The *diameter* of a graph is the maximum distance between two distinct vertices. A (directed) *cycle* is a connected graph where every vertex is incident with one incoming and one outcoming edge. An *acyclic graph* is a graph with no cycles.

B. Formation Graphs

We consider formations that can be represented by acyclic[1] directed graphs. In these graphs, the agents involved are identi£ed by vertices and the leader-following relationships by (directed) edges. The orientation of each edge distinguishes the leader from the follower. Follower controllers implement static state feedback control laws that depend on the state of the particular follower and the states of its leaders.

De£nition II.1 (Formation Control Graph). *A formation control graph $\mathcal{F} = (V, E, S)$ is a directed acyclic graph consisting of:*

- *A £nite set $V = \{v_1, \ldots, v_N\}$ of N vertices and a map assigning to each vertex v_i a control system $\dot{x}_i = f_i(t, x_i, u_i)$ where $x_i \in \mathbb{R}^n$ and $u_i \in \mathbb{R}^m$.*
- *An edge set $E \subset V \times V$ encoding leader-follower relationships between agents. The ordered pair $(v_i, v_j) \triangleq e_{ij}$ belongs to E if u_j depends on the state of agent i, x_i.*
- *A collection $D = \{d_{ij}\}$ of edge speci£cations, de£ning control objectives (setpoints) for each $j : (v_i, v_j) \in E$ for some $v_i \in V$.*

For agent j, the tails of all incoming edges to vertex j represent leaders of j, and their set is denoted by $L_j \subset V$. Vertices v_ℓ of indegree zero represent formation leaders with $v_\ell \in L_F \subseteq V$. Since there are no incoming edges for the vertices in L_F, no formation speci£cations can be de£ned for formation leaders; instead, these agents regulate their behavior so that the formation may achieve some group objectives such as navigation in obstacle environments or tracking reference paths.

Given a speci£cation d_{kj} on edge $(v_k, v_j) \in E$, a setpoint for agent j can be expressed as $x_j^r = x_k - d_{kj}$. For agents with multiple leaders, the speci£cation redundancy can be resolved by projecting the incoming edges speci£cations into orthogonal components:

$$x_j^r = \sum_{k \in L_j} S_{kj}(x_k - d_{kj}) \tag{1}$$

where S_{kj} are projection matrices with $\sum_k \operatorname{rank}(S_{kj}) = n$. Then the error for the closed loop system of agent j is de£ned to be the deviation from the prescribed setpoint $\tilde{x}_j \triangleq x_j^r - x_j$, and the formation error vector is constructed by stacking the errors of all followers:

$$\tilde{x} \triangleq [\cdots \tilde{x}_j \cdots]^T, \quad v_j \in V \setminus L_F$$

Formation leaders are supposed to pursue some group objectives (missions). Consider a formation leader associated with a vertex $v_\ell \in L_F$. If these objectives are known a priori, then they can be encoded in some nominal trajectory, x_ℓ^r, in which case we can de£ne the error for agent ℓ as: $\tilde{x}_\ell = x_\ell^r - x_\ell$. Now consider the input transformation $u_\ell = \tilde{u}_\ell + w_\ell$, and assume a feedback control law $\tilde{u}_\ell(\tilde{x}_\ell)$, which makes the origin of the closed loop system

$$\dot{\tilde{x}}_\ell = \tilde{f}_\ell(t, \tilde{x}_\ell, w_\ell)$$

with $w_\ell = 0$, asymptotically stable. Similarly, if the mission objectives are unspeci£ed, we can set $x_\ell^r = 0$, and assume the existence of an asymptotically stabilizing control law, $\tilde{u}_\ell$, that makes $\dot{\tilde{x}}_\ell = \tilde{f}_\ell(t, \tilde{x}_\ell, 0)$ asymptotically stable. Then, the mission objectives can be realized by means of the input term w_ℓ.

C. Leader-to-Formation Stability

In this section we investigate the stability properties of the formation with respect to all leader inputs w_ℓ or errors $\tilde{x}_\ell$ (in the case where leader control specs have been encoded in x_ℓ^r.) We obtain nonlinear gain estimates that quantify the transient effects of initial errors $\tilde{x}(t_0)$ and the steady state effects of leader inputs w_ℓ, $v_\ell \in L_F$ on the amplitude of the formation error $\tilde{x}$.

De£nition II.2 (LFS). *A formation is called leader-to-formation stable (LFS) if there is a class $\mathcal{KL}$ function β and a class $\mathcal{K}$ function γ such that for any initial formation error $\tilde{x}(0)$ and for any bounded inputs of the formation leaders, $\{w_\ell\}$ the formation error satis£es:*

$$\|\tilde{x}(t)\| \leq \beta(\|\tilde{x}(0)\|, t) + \sum_{\ell \in L_F} \gamma_\ell \left(\sup_{[0,t]} \|w_\ell\| \right) \tag{2}$$

The functions $\beta(r, t)$ and $\gamma_\ell(r)$ are called transient and asymptotic LFS *gains for the formation.*

Leader-to-formation stability builds on the notion of input-to-state stability and it is a 'robustness' property [36], [37]. In this approach, the formation is viewed as a nonlinear operator from the space of leader input/disturbances to the space of the formation internal state. Functions $\beta(r, t)$ and $\gamma_\ell(r)$, in (2)

[1] The case of cycles in a formation graph is treated in [18].

are 'nonlinear gain estimates' quantifying the effect of initial conditions and leader input on formation errors. Inequality (2) provides a safety bound on the formation error. Thus, given a safety speci£cation, and a set of initial conditions, one can estimate an upper bound on the admissible input that can keep the system safe; conversely, given a safety speci£cation and under a particular input regime, a set of initial conditions from which systems trajectories remain safe at all times, can be determined.

Based on alternative characterizations of input-to-state stability [36], De£nition II.2 implies the following:

Corollary II.3. *If a formation is LFS, in the sense of De£nition II.2, then the formation error satis£es:*

$$\lim_{t\to\infty} \|\tilde{x}(t)\| \leq \sum_{\ell\in L_F} \gamma_\ell(\sup \|w_\ell\|)$$

Corollary II.3 establishes the asymptotic LFS gain $\gamma(\sup \|w_\ell\|)$ as an ultimate bound for the formation error. This motivates the de£nition of the following LFS stability measure:

De£nition II.4. *Consider a formation that is LFS. Then the scalar quantity:*

$$P_{LFS} \triangleq \frac{1}{1+\sum_{\ell\in L_F} \gamma_\ell(1)}$$

is called the LFS stability measure of the formation.

As de£ned, P_{LFS} varies in $[0, 1]$. The sum in the denominator of the de£ning equation for the LFS measure gives an estimate of the region in which the steady state formation error will remain, when the inputs to the formation leaders are bounded inside unit balls. The larger the error region grows, the smaller the LFS measure becomes. On the other hand, as the size of the error region shrinks, the performance measure tends to 1.

III. LFS Propagation

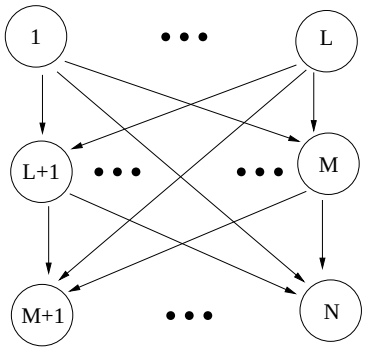

Fig. 1. A generic formation control graph.

In the formation graphs we consider in this paper, all induced subgraphs with N vertices have the form of Figure 1. This means that all cycles in the underlying undirected graph are of order 3. This is done to simplify the analysis, which can be extended to more general interconnection topologies at the expense of added analytical complexity. Assume an enumeration on the induced formation control graph of Figure 1, where the vertices in the £rst row are assigned the numbers $1, \ldots, L$, the vertices in the second are assigned the numbers $L+1, \ldots, M$ and the rest are assigned the numbers $M+1, \ldots, N$. Let the dynamics of the agents be expressed as follows:

$$\dot{x}_\ell = f_\ell(t, x_\ell, u_\ell), \quad \ell \in \{1, \ldots, L\} \tag{3a}$$
$$\dot{x}_i = f_i(t, x_i, u_i), \quad i \in \{L+1, \ldots, M\} \tag{3b}$$
$$\dot{x}_f = f_f(t, x_f, u_f), \quad f \in \{M+1, \ldots, N\} \tag{3c}$$

The agents are driven by control laws of the form:

$$u_\ell = u_\ell(t, x_\ell, \tilde{x}_\ell, w_\ell), \quad \ell \in \{1, \ldots, L\} \tag{4a}$$
$$u_i = u_i(t, x_i, \tilde{x}_i), \quad i \in \{L+1, \ldots, M\} \tag{4b}$$
$$u_f = u_f(t, x_f, \tilde{x}_f), \quad f \in \{M+1, \ldots, N\} \tag{4c}$$

resulting in closed loop error dynamics which can be written as:

$$\dot{\tilde{x}}_\ell = \tilde{f}_\ell(t, \tilde{x}_\ell, v_\ell) \tag{5a}$$
$$\dot{\tilde{x}}_i = \tilde{f}_i(t, \tilde{x}_1, \ldots, \tilde{x}_L, \tilde{x}_i) \tag{5b}$$
$$\dot{\tilde{x}}_f = \tilde{f}_f(t, \tilde{x}_1, \ldots, \tilde{x}_M, \tilde{x}_f) \tag{5c}$$

The main result of the paper is based on the invariance of the LFS property under a broad class of interconnections:

Proposition III.1. *Consider the formation of Figure 1 with closed loop error dynamics given by* (5)*. If* (5b) *is LFS with respect to* $\tilde{x}_1, \ldots, \tilde{x}_L$*:*

$$\|\tilde{x}_i(t)\| \leq \beta_i(\|\tilde{x}(0)\|, t) + \textstyle\sum_{\ell=1}^{L} \gamma_{\ell i}(\sup \|\tilde{x}_\ell\|)$$

and (5c) *is LFS with respect to* $\tilde{x}_1, \ldots, \tilde{x}_M$*:*

$$\|\tilde{x}_f(t)\| \leq \beta_f(\|\tilde{x}_f(0)\|, t) + \textstyle\sum_{i=1}^{M} \gamma_{if}(\sup \|\tilde{x}_i\|)$$

then the induced formation control graph is LFS with respect to $\tilde{x}_1, \ldots, \tilde{x}_L$*:*

$$\|\tilde{x}(t)\| \leq \beta(\|\tilde{x}(0)\|, t) + \textstyle\sum_{\ell=1}^{L} \gamma_\ell(\sup \|\tilde{x}_\ell\|)$$

with $\tilde{x} := (\tilde{x}_{L+1}, \ldots, \tilde{x}_N)$ *and*

$$\beta(r,t) = \textstyle\sum_{f=M+1}^{N} \Big\{ \sum_{i=L+1}^{M} \Big[\gamma_{if}\Big(4\beta_i\big(2\beta_i(\|\tilde{x}(0)\|, 0), \frac{t}{2}\big)\Big) + \beta_i\big(\|\tilde{x}(0)\|, t\big)\Big] + \beta_f\Big(2\beta_f\big(\|\tilde{x}(0)\|, \tfrac{t}{2}\big) + 2\textstyle\sum_{i=L+1}^{M} \gamma_{if}\big(2\beta_i(\|\tilde{x}(0)\|, 0)\big), t\Big)\Big\} \tag{6a}$$

$$\gamma_\ell(r) = \textstyle\sum_{f=M+1}^{N} \Big[\sum_{i=L+1}^{M} \gamma_{if}\big(2L\gamma_{\ell i}(r)\big) + \gamma_{\ell f}(r) + \beta_f\Big(2L\big(\sum_{\ell=1}^{L} \gamma_{\ell f}(r) + \sum_{i=L+1}^{M} \gamma_{if}(2L\gamma_{\ell i}(r))\big), 0\Big) + \sum_{i=L+1}^{M} \gamma_{\ell i}(r) + \sum_{i=L+1}^{M} \gamma_{if}\Big(4\beta_i\big(2L\gamma_{\ell i}(r), 0\big)\Big)\Big]. \tag{6b}$$

Proof. See Appendix. □

In the case where the agent dynamics are linear, then the conditions for LFS are automatically satis£ed. The following

Proposition takes into account the linearity of the gain functions and provide less conservative bounds than those obtained by applying (6) to the linear case. The linear version of (3) has the following form:

$$\begin{aligned}\dot{x}_\ell &= Ax_\ell + Bu_\ell, \quad \ell \in \{1,\dots,L\}\\ \dot{x}_i &= Ax_i + Bu_i, \quad i \in \{L+1,\dots,M\}\\ \dot{x}_f &= Ax_f + Bu_f, \quad f \in \{M+1,\dots,N\},\end{aligned}$$

along with the feedback control laws:

$$u_i = K_i\tilde{x}_i + e_i \tag{7a}$$
$$u_f = K_f\tilde{x}_f + e_f, \tag{7b}$$
$$u_\ell = K_\ell\tilde{x}_\ell + e_\ell, \tag{7c}$$

where K_i, K_f, and K_ℓ are such that $(A_s - B_sK_s)$, $s \in \{1,\dots,N\}$ are Hurwitz, and e_i, e_ℓ and e_f satisfy:

$$B_ie_i = -A_ix_i^r, \quad B_fe_f = -A_fx_f^r, \quad B_\ell e_\ell = -A_\ell x_\ell^r$$

These ensure that the control inputs of each follower can provide the appropriate feedforward action to track the leader. Application of (7) results in closed loop error dynamics that can be written as:

$$\dot{x}_\ell = -(A_\ell - B_\ell K_\ell)\tilde{x}_\ell, \tag{8a}$$
$$\dot{\tilde{x}}_i = (A_i - B_iK_i)\tilde{x}_i + \dot{x}_i^r \tag{8b}$$
$$\dot{\tilde{x}}_f = (A_f - B_fK_f)\tilde{x}_f - \sum_{i=L+1}^{M} S_{if}(A_i - B_iK_i)\tilde{x}_i, \tag{8c}$$

This model is equivalent to the one used for a string of LTI systems in [38]. In this case, the LFS gains are as follows:

Proposition III.2. *Consider the formation of Figure 1 where the closed loop error dynamics of the agents are given by* (8)*. Then,* (8) *is* LFS *with respect to* $\tilde{x}_1,\dots,\tilde{x}_L$*:*

$$\|\tilde{x}(t)\| \le \bar{\beta}\,\|\tilde{x}(0)\|\,e^{-\mu t} + \textstyle\sum_{\ell=1}^{L}\bar{\gamma}_\ell \sup\|\tilde{x}_\ell\|$$

where $\theta \in (0,1)$ *is a parameter,* $\mu = \frac{1-\theta}{4\max\{\lambda_M[P_i],\lambda_M[P_f]\}}$*,* $\lambda_M[\cdot]$ *and* $\lambda_m[\cdot]$ *are the largest and smallest eigenvalues of a matrix, respectively,*

$$\bar{\beta} \triangleq \sum_{i=L+1}^{M}\Big[\sum_{f=M+1}^{N}\big(\bar{\beta}_f^2 + (\bar{\beta}_i+\bar{\beta}_f)\bar{\beta}_i\bar{\gamma}_{if}\big) + \bar{\beta}_i\Big] \tag{9a}$$

$$\bar{\gamma}_\ell \triangleq \sum_{f=M+1}^{N}\big[(1+\bar{\beta}_f)\bar{\gamma}_{\ell f} + \sum_{i=L+1}^{M}(\bar{\beta}_f+\bar{\beta}_i+1)\bar{\gamma}_{if}\bar{\gamma}_{\ell i} + \bar{\gamma}_{\ell i}\big] \tag{9b}$$

with $\bar{\beta}_r = \left(\frac{\lambda_M[P_r]}{\lambda_m[P_r]}\right)^{\frac{1}{2}}$*, for* $r = 1,\dots,N$*,* $\bar{\gamma}_{ji} = \frac{2(\lambda_M[P_i])^{\frac{3}{2}}\lambda_M[A_j-B_jK_j]}{(\lambda_m[P_i])^{\frac{1}{2}}\theta}$*, and each* P_j *satisfying:*

$$P_j(A_j - B_jK_j) + (A_j - B_jK_j)^TP_j = -I$$

Proof. See Appendix. □

IV. Graph Propagation Matrix Equations

For linear systems, the LFS gain propagation equations (9) can be encoded in recursive matrix equations, in which the formation graph structure appears explicitly in the form of the graph adjacency matrix. The recursion is based on the property of the powers of the adjacency matrix to give the number of paths of length equal to the exponent between two vertices in the graph [35]. By labeling the edges of the graph with the LFS gains associated with the particular edge, we are able to propagate the gains through the graph and obtain a sequence of matrices that express the LFS gains of all paths inside the formation graph.

Consider the adjacency matrix A of $\mathcal{G}$:

$$A = [a_{ij}], \text{ where } \begin{cases} a_{ij} = 1, \text{ if } (v_i, v_j) \in E \\ a_{ij} = 0, \text{ otherwise} \end{cases}$$

and de£ne the matrices $\Gamma, B \in \mathbb{R}^{|\mathcal{V}|\times|\mathcal{V}|}$ as follows:

$$B = [b_{ij}], \text{ where } \begin{cases} b_{ij} = \bar{\beta}_j, \text{ if } a_{ij} = 1 \\ b_{ij} = 0, \text{ otherwise} \end{cases} \tag{10}$$

$$G = [g_{ij}], \text{ where } \begin{cases} g_{ij} = \bar{\gamma}_{ji}, \text{ if } a_{ij} = 1 \\ g_{ij} = 0, \text{otherwise} \end{cases} . \tag{11}$$

Obviously, matrices B and G provide the transient and asymptotic LFS gains of all paths of length one (edges) in the formation graph. Thus we de£ne:

$$B_1 = B, \qquad G_1 = G,$$

respectively, where the subscript denotes the length of the path. Then the LFS gains of all longer paths in the formation graph can be computed through the recursive procedure described in the following Proposition:

Proposition IV.1. *Consider a formation control graph* $\mathcal{G}$ *with adjacency matrix* A *and matrices* B*,* G *de£ned by* (10) *and* (11)*, respectively. Then, the asymptotic and transient* LFS *gains of paths of length* $k > 1$ *between two vertices* $v_i, v_j \in \mathcal{V}$ *are given recursively as the* (i,j) *elements of matrices*

$$\begin{aligned}G_k &= G(G_{k-1}\circ B_{k-1}) + GG_{k-1} + (G\circ B)G_{k-1}\\ &\quad + GA^{k-1} + G\circ(AB_{k-1} + A^k)\end{aligned} \tag{12a}$$
$$\begin{aligned}B_k &= A(B_{k-1}\circ B_{k-1}) + BA^{k-1} + (B\circ B)G_{k-1}\\ &\quad + B(G_{k-1}\circ B_{k-1}),\end{aligned} \tag{12b}$$

respectively, where $\circ$ *denotes the Schur (elementwise) matrix product. Moreover, the recursion terminates after* $d \le |\mathcal{V}| - 1$ *steps, where* d *is the diameter of the formation graph* $\mathcal{G}$*.*

Proof. See Appendix. □

V. Relation to Alternative Methodologies

The framework of string and mesh stability provides an alternative way of analyzing the stability of interconnected systems. Mesh stability guarantees error attenuation and establishes stability properties which are preserved when the group is augmented. LFS, on the other hand, models the effect of leader

inputs and can be used to address issues related to safety and performance.

Although both notions re¤ect some robustness properties of the system, due structural perturbations in the former case and input disturbances in the latter, the similarities seem to end here:

- mesh stability ensures scalable stability properties which are independent of system size whereas LFS relates stability properties with initial conditions, input and error speci£cations, and system size and interconnection topology;
- mesh stability establishes the convergence of interconnection errors to zero while LFS provides ultimate bounds that depend on initial conditions and inputs;
- in a mesh stable system errors attenuate due to 'weak interaction' conditions while in an LFS system errors can increase but their ampli£cation is quanti£ed via nonlinear gain estimates.
- there is no notion of input in mesh stability;
- LFS nonlinear systems are generally not mesh stable;

Although LFS and mesh stability are generally incomparable, one can establish a link between them, in the sense that mesh stability of the unforced system may, under some sector conditions on the input vector £elds, imply local LFS. In this respect, it is possible to introduce inputs in a mesh stable system and analyze their effect on the size of the errors observed.

Proposition V.1. *For a look ahead system, af£ne in control:*

$$\dot{x}_1 = f_1(t,x_1) + g_1(t,x_1)u_1 \tag{13a}$$
$$\dot{x}_2 = f_2(t,x_2,x_1) + g_2(t,x_2,x_1)u_2 \tag{13b}$$
$$\vdots$$
$$\dot{x}_N = f_N(t,x_N,\ldots,x_1) + g_N(t,x_N,\ldots,x_1)u_N \tag{13c}$$

If for $u_i = 0$, $i = 1,\ldots,N$, (13) *is asymptotically mesh stable at the origin* $x \triangleq (x_1,\ldots,x_N) = 0$, *and there are class-*$\mathcal{K}$ *functions* $\zeta_i(\cdot)$ *such that*

$$\|g_i(t,x_i,\ldots,x_1)\| \leq \zeta(\|x\|) \triangleq \max_{r,i}\{\zeta_i(r)\}, \quad i = 1,\ldots,N$$

then there is a neighborhood of the origin, $D = \{x : \|x\| \leq r\}$ *where* (13) *is* LFS.

Proof. See Appendix. □

The converse, however, is not true. If (13) is LFS, setting $u_i = 0$ does not necessarily mean that $\|x_i(t)\|_\infty \leq \|x(t)\|_\infty^{i-1}$, which is required for mesh stability [30]. Suf£cient conditions for mesh stability include global Lipschitz continuity of the system vector £elds with respect to coupling terms and exponential stability of the unforced dynamics [30]. These conditions may not necessarily be satis£ed in LFS systems [21].

VI. Applications

A. LFS in Mobile Robot Formations

The results of Section III can be applied to formations of nonholonomic mobile robots. We borrow the application example of [15] and we show that the resulting edge error dynamics are LFS. For each nonholonomic mobile robot we consider the following kinematic model:

$$\dot{x}_i = v_i\cos\theta_i, \qquad \dot{y}_i = v_i\sin\theta_i \qquad \dot{\theta}_i = \omega_i. \tag{14}$$

where (x,y,θ) is the position and orientation of mobile robot i, and v_i, ω_i are the translational and rotational velocity control inputs. For a triple of robots i, j and k where j is supposed

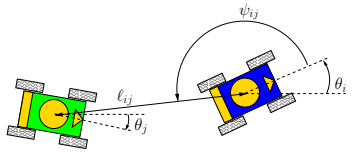

Fig. 2. Leader following using a separation-bearing controller.

to follow i and i is supposed to follow k, the speci£cation for the leader-follower relationship can be expressed in terms of the separation distance ℓ and the relative bearing ψ (Figure 2) which e.g. for the $i-j$ pair can be written as:

$$h_{ij} = (\ell_{ij}^d - \ell_{ij}, \psi_{ij}^d - \psi_{ij}) \triangleq (\tilde{\ell}_{ij}, \tilde{\psi}_{ij}) = 0.$$

where ℓ_{ij}^d and ψ_{ij}^d are constant speci£cation parameters. Taking h_{ij} as an output, the dynamics of the $i-j$ leader-follower pair can be expressed in new coordinates as:

$$\begin{bmatrix}\dot{\tilde{\ell}}_{ij}\\ \dot{\tilde{\psi}}_{ij}\\ \dot{\phi}_{ij}\end{bmatrix} = \begin{bmatrix}\cos\psi_{ij} & 0\\ \frac{-\sin\psi_{ij}}{\ell_{ij}} & 1\\ 0 & 1\end{bmatrix}\begin{bmatrix}v_i\\ \omega_i\end{bmatrix} - \begin{bmatrix}\cos(\phi_{ij}+\psi_{ij}) & d\sin(\phi_{ij}+\psi_{ij})\\ \frac{-\sin(\phi_{ij}+\psi_{ij})}{\ell_{ij}} & \frac{d\cos(\phi_{ij}+\psi_{ij})}{\ell_{ij}}\\ 0 & -1\end{bmatrix}\begin{bmatrix}v_j\\ \omega_j\end{bmatrix}$$

where d is a modeling parameter and $\phi_{ij} = \theta_i - \theta_j$. Using input-output feedback linearization:

$$\begin{bmatrix}v_j\\ \omega_j\end{bmatrix} = \begin{bmatrix}\cos(\phi_{ij}+\psi_{ij}) & -\ell_{ij}\sin(\phi_{ij}+\psi_{ij})\\ \frac{\sin(\phi_{ij}+\psi_{ij})}{d} & \frac{\ell_{ij}\cos(\phi_{ij}+\psi_{ij})}{d}\end{bmatrix}\begin{bmatrix}k_1^j\tilde{\ell}_{ij}\\ k_2^j\tilde{\psi}_{ij}\end{bmatrix} \tag{15a}$$

$$\begin{bmatrix}v_i\\ \omega_i\end{bmatrix} = \begin{bmatrix}\cos(\phi_{ki}+\psi_{ki}) & -\ell_{ki}\sin(\phi_{ki}+\psi_{ki})\\ \frac{\sin(\phi_{ki}+\psi_{ki})}{d} & \frac{\ell_{ki}\cos(\phi_{ki}+\psi_{ki})}{d}\end{bmatrix}\begin{bmatrix}k_1^i\tilde{\ell}_{ki}\\ k_2^i\tilde{\psi}_{ki}\end{bmatrix} \tag{15b}$$

the interconnection error dynamics can take the form:

$$\begin{bmatrix}\dot{\tilde{\ell}}_{ij}\\ \dot{\tilde{\psi}}_{ij}\end{bmatrix} = -\begin{bmatrix}k_1^j\tilde{\ell}_{ij}\\ k_2^j\tilde{\psi}_{ij}\end{bmatrix} - \begin{bmatrix}-\cos\psi_{ij}\cos(\phi_{ki}+\psi_{ki}) & \ell_{ki}\cos\psi_{ij}\sin(\phi_{ki}+\psi_{ki})\\ \frac{\sin\psi_{ij}\cos(\phi_{ki}+\psi_{ki})}{\ell_{ij}} - \frac{\sin(\phi_{ki}+\psi_{ki})}{d} & -\frac{\ell_{ki}\sin\psi_{ij}\sin(\phi_{ki}+\psi_{ki})}{\ell_{ij}} - \frac{\ell_{ki}\cos(\phi_{ki}+\psi_{ki})}{d}\end{bmatrix}\begin{bmatrix}k_1^i\tilde{\ell}_{ki}\\ k_2^i\tilde{\psi}_{ki}\end{bmatrix} \tag{16}$$

The internal dynamics of ϕ_{ij} can be shown to be stable [15]. Then, using $V_{ij} = \frac{1}{2k_1^j}\|\tilde{\ell}_{ij}\|^2 + \frac{1}{2k_2^j}\|\tilde{\psi}_{ij}\|^2$ as a Lyapunov function for (16), and denoting $(\tilde{\ell}_{ij},\tilde{\psi}_{ij})^T$ by $\tilde{z}_{ij}$, we can arrive at:

$$\dot{V}_{ij} \leq -\|\tilde{z}_{ij}\|^2 + \|\tilde{z}_{ij}\|\begin{bmatrix}\frac{1}{k_1^j} & 0\\ 0 & \frac{1}{k_2^j}\end{bmatrix}\begin{bmatrix}-\cos\psi_{ij} & 0\\ \frac{\sin\psi_{ij}}{\ell_{ij}} & -1\end{bmatrix}\left\|\begin{pmatrix}v_i\\ \omega_i\end{pmatrix}\right\|$$

which yields for $\xi \in (0,1)$:

$$\dot{V}_{ij} \leq -(1-\xi)\|\tilde{z}_{ij}\|^2, \forall\, \|\tilde{z}_{ij}\| \geq \frac{\max\{k_1^i,k_2^i\}(d+\ell_{ki}^d+\|\tilde{z}_{ki}\|)\|\tilde{z}_{ki}\|}{\xi d\min\{k_1^j,k_2^j\}}$$

Then follows that: $\|\tilde{z}_{ij}\| \leq \beta_{ij}(\|\tilde{z}_{ij}(0)\|, t) + \gamma_{ij}(\sup\|\tilde{z}_{ki}\|)$, where

$$\beta_{ij}(r,t) = r\sqrt{\frac{\max\{k_1^j,k_2^j\}}{\min\{k_1^j,k_2^j\}}}e^{-(1-\xi)\min\{k_1^j,k_2^j\}t} \tag{17a}$$

$$\gamma_{ij}(r) = \frac{\max\{k_1^j,k_2^j\}^{\frac{1}{2}}\max\{k_1^i,k_2^i\}(d+\ell_{ki}^d+r)r}{\xi d\min\{k_1^j,k_2^j\}^{\frac{3}{2}}} \tag{17b}$$

establishing the LFS property of the leader-follower pair.

The simulated response of a string of ten mobile robots with dynamics described by (14), is steered using the leader-follower controllers (15) is depicted in Figures 3-4. Figure 3 shows the paths of the £rst and the last robots in the string, in an effort to follow a sinusoidal reference trajectory while maintaining the shape of a straight line. Error propagation causes large overshoot for the last follower. Figure 4 presents the time evolution of the formation errors related to separation and bearing. After an initial transient period, the errors remain bounded inside a certain region that depends on the magnitude of the velocity along the reference trajectory.

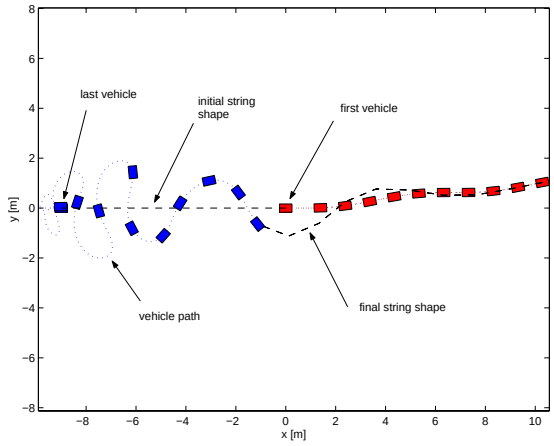

Fig. 3. A string of 10 vehicles tracking a sinusoidal trajectory.

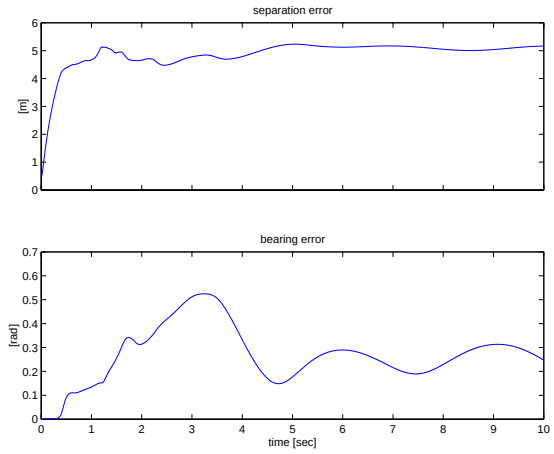

Fig. 4. Formation errors for the string of 10 vehicles.

B. Architecture Comparison

In this section we will £rst turn our attention to a formation of three mobile robots (Figure 5). We will use LFS to assess and numerically verify the stability properties of three different formation architectures, based on (16). We compare the three architectures depicted in Figures 6 and 8. In the simulation runs, the formation leader, robot 1 has to follow a circular reference trajectory, while the other robots have to remain in a straight line behind the leader. The parameter values selected are $\ell_{12}^d = 0.75[m]$ $\psi_{12}^d = \pi[rad]$, $\ell_{23}^d = 0.75[m]$, $\psi_{23}^d = \pi[rad]$, $\ell_{13}^d = 1.75[m]$, $d = 0.25[m]$ and the controller gains are set to $k_1 = 10$, $k_2 = 10$ for all robots.

The cascade formation of Figure 6 has an LFS asymptotic gain: $\gamma(r) = 8r(r+2) + 256r(r+2)[2+16r(2+r)] + 512r(2+r)[2+64r(2+r)]$ and an LFS performance measure $P_{LFS} = 3.367 \times 10^{-7}$. For the parallel formation of Figure 8 we have $\gamma(r) = 16r(2+r)$ and $P_{LFS} = 0.98$, which indicate a signi£cant qualitative difference in performance. This difference is depicted in Figures 7 and 9, where it is obvious that in parallel formation, the robots are able to move in alignment more accurately. Although the gain estimates calculated are crude, having to account for the worst case, there are still indicative of the stability properties of the system. Indeed, as it can be seen in Figure VI-B, the parallel formation clearly outperforms the cascade architecture.

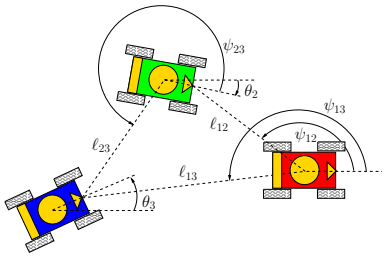

Fig. 5. Three mobile robots using separation-bearing controllers.

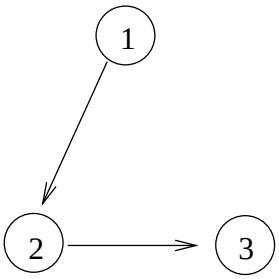

Fig. 6. Cascade formation.

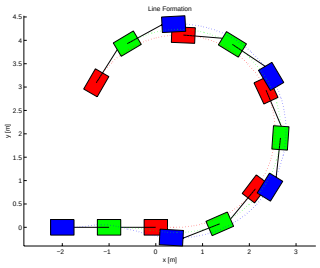

Fig. 7. Robot paths for the cascade formation.

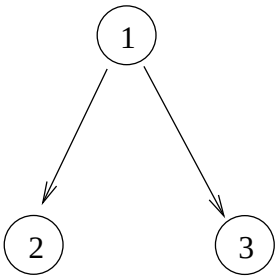

Fig. 8. Parallel formation.

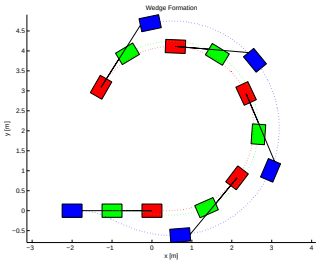

Fig. 9. Robot paths for the parallel formation.

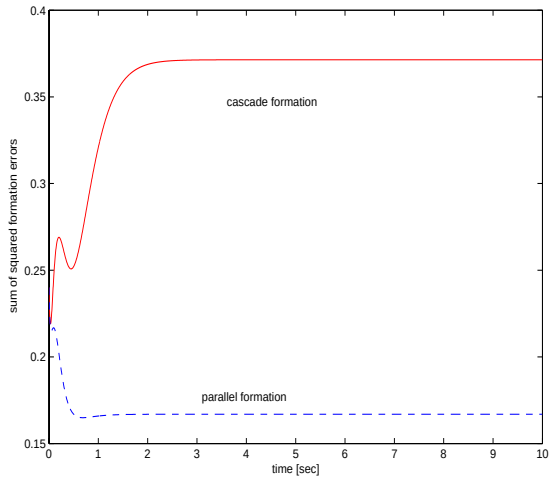

Fig. 10. Formation error evolution for the two formation architectures.

Consider now the formation depicted in Figure VI-B. All robots are thought to use the controllers (15), with the only difference that the vehicle 3 uses higher feedback gains compared to all the others. In view of the increased performance capabilities of robot 3, one may consider assigning robots $5, 6$, and 7 to follow 3. However, an LFS analysis reveals that such a change will in fact increase the magnitude of the formation errors: assume that $k_1^i = kI_2 = k$, for $i = \{1, 2, 4, 5, 6, 7\}$ and $k_1^3 = k_2^3 = k' > k$. Suppose that collision avoidance imposes a maximum allowable error bound, $\|r\| < R$. Then the LFS gains of (17) can be overapproximated as follows:

$$\beta_{ij}(r,t) = re^{-(1-\xi)k^j t}, \tag{18a}$$

$$\gamma_{ij}(r) = \frac{k^i}{k^j}\left(\frac{d+\ell+R}{\xi d}\right) r \tag{18b}$$

With $\xi = 0.5$, $d = 0.25$ and $\ell = 0.75$, from (18) we derive:

Nearest neighbor following	Following 3
$\gamma_{25} = 2(1+R)r$	$\gamma_{25} = 2\frac{k'}{k}(1+R)r$
$\gamma_{36} = 2\frac{k'}{k}(1+R)r$	$\gamma_{36} = 2\frac{k'}{k}(1+R)r$
$\gamma_{47} = 2(1+R)r$	$\gamma_{47} = 2\frac{k'}{k}(1+R)r$

Since $k' > k$, robots 5 and 7 will exhibit larger errors in the interconnection of Figure VI-B compared to those expected in the interconnection of Figure VI-B. This is because higher feedback gains for robot 3 result to larger control inputs which propagate into robots 5 and 7, increasing their formation errors.

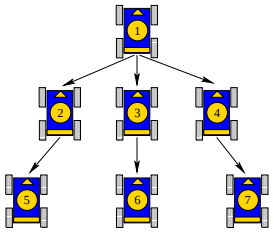

Fig. 11. Nearest neighbor following.

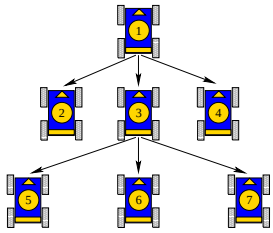

Fig. 12. Following the fastest robot.

C. Safety Speci£cations

Leader-to-Formation Stability gains can be used to check and implement safety speci£cations that are related to formation errors. In the example of this Section, we consider a formation of three robots connected in cascade via the separation-bearing controllers (15). The group is supposed maneuver maintaining a triangular shape for which the faces must not exceed a certain distance. This will ensure that the robots move in a tight formation, in the same way as £ghters when ¤ying in formation have to maintain certain patterns to avoid detection by enemy radars.

The leader of the formation is to follow a reference trajectory. The time parameterization of the reference trajectory de£nes a desired velocity for the leader. This reference velocity can be regarded as an input to the formation and as such it will affect the size of the formation errors. If the magnitude of this velocity were a design parameter, then a question that arises is whether one can select an appropriate value to ensure that the formation can track the reference trajectory without violating its safety speci£cation.

The formation motion is simulated £rst for the case where the reference velocity is set to a constant value: $\|u_\ell\| = 1$. The robot paths are given in Figure VI-C. A circle of radius $\rho = 1.5[m]$ around the formation leader marks the boundary of the region in which the followers should be for the group to satisfy the safety speci£cation. Due to the magnitude of the reference velocity for the leader, the formation shape is distorted and the last follower in the string exhibits an unacceptable error, which forces it to remain outside the safe region.

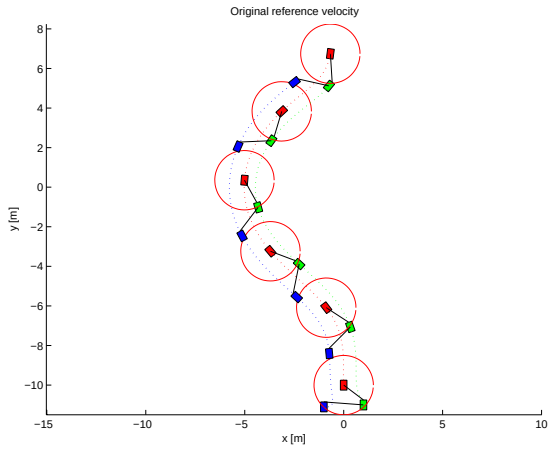

Fig. 13. Formation input not satisfying safety spec.

Based on the fact that the distance between the last follower and the leader should not exceed $1.5[m]$, we can determine the largest allowable formation error: $\tilde{x}_{\max} = 0.5829$. Using the LFS gain estimates (18), with $R = 0.5829$, $k_1 = k_2 = 10$ and $\xi = 0.5$, we derive a formation asymptotic gain: $\bar{\gamma}_\ell = 1721.73$. This implies that in order for $\tilde{x} \leq \tilde{x}_{\max}$ it suf£ces to have $\|u_\ell\| \leq 0.000338$. Then the reference speed for the leader is set to $\|u_\ell\| \triangleq 0.0001$ and the formation motion is simulated again and depicted in Figure VI-C, where it is clear that the safety speci£cation is now satis£ed.

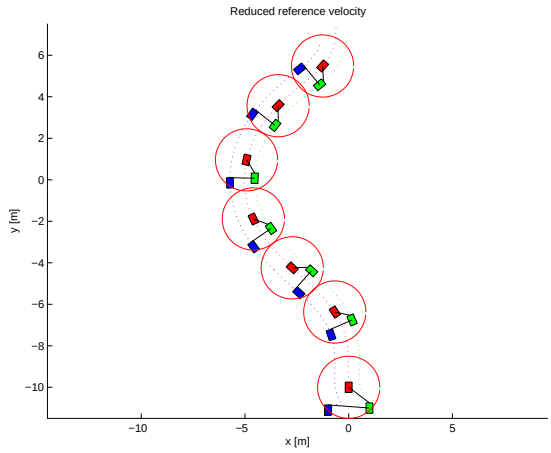

Fig. 14. Slowing down the formation to satisfy safety spec.

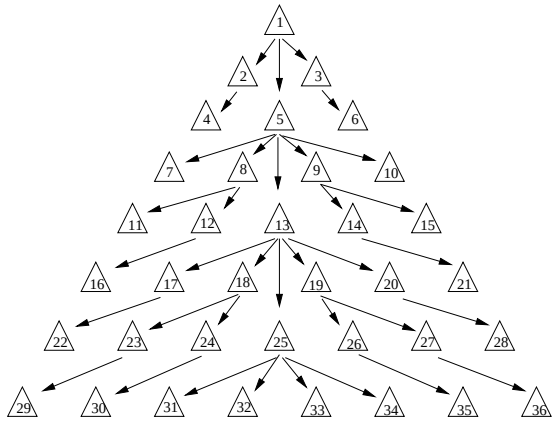

Fig. 15. Gain computation in large formations.

D. Gain Computation

One of the major considerations when dealing with large scale interconnected systems such as large vehicle formations, is the ability to compute the gain estimates ef£ciently, regardless of the size of the system. For nonlinear systems, due to their inherent complexity, LFS gain computation using (6) is cumbersome and does not scale well. The conclusions that can be drawn in the case of large scale vehicle formations are basically qualitative: one knows that the LFS property of individual subsystems ensures the continuous dependence of the size of the formation errors on the amplitude of the leaders excitation. Figure 3 shows the vehicle paths in a string of ten, with closed loop dynamics described by (16). Figure 4 gives the formation error evolution with respect to time in which, due to the absence of an appropriate norm on $SE(2)$, we chose to plot the position and orientation errors separately. Figures 3-4 show how LFS can ensure boundedness of errors and continuous dependence of system trajectories on leader input.

In the remaining of this section we will demonstrate the use of equations (12) to assess the stability properties of the formation depicted in Figure VI-D. To apply equations (12) we consider a linear overapproximation of the LFS gains in the sense of (18) and assume $\bar{\beta}_{ij} = 1.2$, $\bar{\gamma}_{ij} = 0.2$ for any pair of leader i and follower j with $i, j \in \{1, \ldots, 36\}$. In this formation graph, the largest path is of length 5. The computation process terminates after 6 steps, yielding an LFS performance measure: $P_{LFS} = \left(1 + \sum_{j=1}^{3} 6\bar{\gamma}_{1j}\right)^{-1} = 772.952^{-1}$

VII. Conclusion

LFS is a stability property of formations that are based on leader-following which quanti£es the propagation of the input of the formation leaders to the interconnection network of the group and captures its effects on the magnitude of the errors observed. It provides performance measures that can be calculated analytically, and allows the calculation of worst case ultimate error bounds. which can be used to check the design against safety speci£cations. The intuitive fact that performance deteriorates as the graph that represents the formation interconnections increases in diameter, can now be formally justi£ed. LFS can be used as an analysis tool to assess the performance and robustness capabilities of different interconnection topologies and expose weaknesses in the design of the formation architecture in the form of error amplifying interconnections. Finally, the worst case ultimate error bounds obtained by LFS can be used to check a particular formation design against error-related safety speci£cations.

Acknowledgments

This research is partially supported under DARPA MICA Contract Number N66001-01-C-8076, and by DARPA/AFRL Software-Enabled Control Grant F33615-01-C-1848.

References

[1] D. Swaroop and J. K. Hedrick, “Sting stability of interconnected systems,” *IEEE Transactions on Automatic Control*, vol. 41, pp. 349–357, March 1996.

[2] T. Balch and R. Arkin, “Behavior-based formation control for multirobot systems,” *IEEE Transactions on Robotics and Automation*, vol. 14, no. 12, 1998.

[3] P. Ögren, E. Fiorelli, and N. E. Leonard, “Formations with a mission: Stable coordination of vehicle group maneuvers,” in *Proceedings of the 15^{th} International Symposium on Mathematical Theory of Networks and Systems*, (Notre Dame, IN), August 2002.

[4] H. G. Tanner, S. G. Loizou, and K. J. Kyriakopoulos, “Nonholonomic navigation and control of multiple mobile manipulators,” *IEEE Transactions on Robotics and Automation*, vol. 19, pp. 53–64, February 2003.

[5] T. Sugar, J. Desai, V. Kumar, and J. P. Ostrowski, “Coordination of multiple mobile manipulators,” in *Proceedings of IEEE International Conference on Robotics Automation*, vol. 3, pp. 3022–2027, May 2001.

[6] M. Mesbahi and F. Hadaegh, “Formation ¤ying of multiple spacecraft via graphs, matrix inequalities, and switching,” *AIAA Journal of Guidance, Control and Dynamics*, vol. 24, pp. 369–377, March 2001.

[7] R. W. Beard, J. Lawton, and F. Y. Hadaegh, “A coordination architecture for spacecraft formation control,” *IEEE Transactions on Control Systems Technology*, vol. 9, pp. 777–790, November 2001.

[8] C. R. McInnes, “Autonomous ring formation for a planar constellation of satellites,” *AIAA Journal of Guidance Control and Dynamics*, vol. 18, no. 5, pp. 1215–1217, 1995.

[9] F. Giulietti, L. Pollini, and M. Innocenti, “Autonomous formation ¤ight,” *IEEE Control Systems Magazine*, vol. 20, no. 6, pp. 34–44, 2000.

[10] D. J. Stilwell and B. E. Bishop, “Platoons of underwater vehicles,” *IEEE Control Systems Magazine*, pp. 45–52, 2000.

[11] S. K. Maurice Martin, Pete Klupar and J. Winter, “Techsat 21 and revolutionizing space missions using microsatellites,” in *15^{th} USU/AIAA*, (Logan, Utah), August 2001.

[12] K.-H. Tan and M. A. Lewis, “Virtual structures for high-precision cooperative mobile robot control,” *Autonomous Robots*, vol. 4, pp. 387–403, October 1997.

[13] R. Olfati-Saber and R. M. Murray, "Distributed structural stabilization and tracking for formations of dynamic multi-agents," in *Proceedings of the IEEE Conference on Decision and Control*, (Las Vegas, NV), pp. 209–215, December 2002.

[14] P. N. B. Tolga Eren and A. S. Morse, "Closing ranks in vehicle formations based on rigidity," in *Proceedings of the IEEE Conference on Decision and Control*, (Las Vegas, NV), pp. 2959–2964, December 2002.

[15] A. K. Das, R. Fierro, and V. Kumar, *Control graphs for robot networks*, vol. Cooperative Control and Optimization of *Applied Optimization*, ch. 4, pp. 55–73. Kluwer Academic Press, 2002.

[16] P. Tabuada, G. J. Pappas, and P. Lima, "Feasible formations of multi-agent systems," in *Proceedings of the American Control Conference*, (Arlington, VA), pp. 56–61, June 2001.

[17] J. A. Fax and R. M. Murray, "Information ¤ow and cooperative control of vehicle formations," in *Proceedings of the 15th IFAC World Congress*, (Barcelona, Spain), pp. 2360–2365, July 2002.

[18] H. Tanner, V. Kumar, and G. Pappas, "Stability properties of interconnected vehicles," in *Proceedings of the 15th International Symposium on Mathematical Theory of Networks and Systems*, (Notre Dame, IN), August 2002.

[19] J. P. Desai, J. P. Ostrowski, and V. Kumar, "Modeling and control of formations of nonholonomic mobile robots," *IEEE Transactions on Robotics and Automation*, vol. 17, no. 6, pp. 905–908, 2001.

[20] R. Fierro, A. Das, V. Kumar, and J. P. Ostrowski, "Hybrid control of formation of robots," in *IEEE Int. Conf. Robot. Automat., ICRA01*, May 2001.

[21] H. G. Tanner, G. J. Pappas, and V. Kumar, "Input-to-state stability on formation graphs," in *Proceedings of the IEEE International Conference on Decision and Control*, (Las Vegas, NV), December 2002.

[22] M. Egerstedt and X. Hu, "Formation constrained multi-agent control," in *Proceedings of the IEEE Conference on Robotics and Automation*, (Seoul, Korea), pp. 3961–3966, May 2001.

[23] N. E. Leonard and E. Fiorelli, "Virtual leaders, arti£cial potentials and coordinated control of groups," in *Proceedings of the IEEE International Conference on Decision and Control*, (Orlando, FL), pp. 2968–2973, December 2001.

[24] R. D'Andrea and G. E. Dullerud, "Distributed control of spatially interconnected systems," *Transactions on Automatic Control (submitted)*, 2002.

[25] R. Fierro, A. Das, V. Kumar, and J. Ostrowski, "Hybrid control of formations of robots," in *Proceedings of the IEEE International Conference on Robotics and Automation*, (Seoul, Korea), pp. 157–162, May 2001.

[26] L. E. Peppard, "String stability of relative-motion PID vehicle control systems," *IEEE Transactions on Automatic Control*, pp. 579–581, October 1974.

[27] S. Sheikholeslam and C. Desoer, "Longitudinal control of a platoon of vehicles," in *Proceedings of the American Control Conference*, vol. 1, pp. 291–297, May 1990.

[28] K. C. Chu, "Decentralized control of high speed vehicle strings," *Transportation Science*, vol. 8, pp. 361–383, 1974.

[29] D. Swaroop, J. Hedrick, C. Chien, and P. Ioannou, "A comparison of spacing and headway control laws for automatically controlled vehicles," *Vehicle System Dynamics*, vol. 23, pp. 597–625, 1994.

[30] A. Pant, P. Seiler, and K. Hedrick, "Mesh stability of look-ahead interconnected systems," *IEEE Transactions on Automatic Control*, vol. 47, pp. 403–407, Feb. 2002.

[31] R. M. Murray, K. J. Åström, S. P. Boyd, R. W. Brockett, and G. Stein, "Future directions in control in an information-rich world," *IEEE Control Systems Magazine*, 2003. to appear.

[32] E. D. Sontag and Y. Wang, "On characterizations of the input-to-state stability property," *Systems & Control Letters*, no. 24, pp. 351–359, 1995.

[33] M. Krstić, I. Kanellakopoulos, and P. Kokotović, *Nonlinear and Adaptive Control Design*. John Willey and Sons, 1995.

[34] A. Isidori, *Nonlinear Control Systems II*. Communications and Control Engineering, Springer, 1999.

[35] C. Godsil and G. Royle, *Algebraic Graph Theory*. Graduate Texts in Mathematics; 207, Springer, 2001.

[36] E. Sontag, "On the input-to-state stability property," *European Journal of Control*, vol. 1, pp. 24–36, 1995.

[37] E. Sontag, "Smooth stabilization implies coprime factorization," *IEEE Transactions on Automatic Control*, vol. 34, pp. 435–443, 1989.

[38] D. Swaroop, "A note about the stability of a string of LTI systems," *ASME Journal of Dynamic Systems, Measurement and Control*, vol. 124, pp. 472–475, September 2002.

[39] R. A. Horn and C. R. Johnson, *Topics in Matrix Analysis*. Cambridge University Press, 1991.

APPENDIX

Proof of Proposition III.1

For the generic formation of Figure 1, note that LFS of each follower f with respect to $\tilde{x}_k$, $k = 1, \ldots, M$, for the time interval $[0, t/2]$ and $f = M+1, \ldots, N$ yields:

$$\left\|\tilde{x}_f(\tfrac{t}{2})\right\| \leq \beta_f\left(\left\|\tilde{x}_f(0)\right\|, \tfrac{t}{2}\right) + \sum_{k=1}^{M} \gamma_{kf}(\sup_{[0,\frac{t}{2}]} \|\tilde{x}_k\|), \quad (19)$$

$$\|\tilde{x}_f(t)\| \leq \beta_f\left(\left\|\tilde{x}_f(\tfrac{t}{2})\right\|, t\right) + \sum_{k=1}^{M} \gamma_{kf}(\sup_{[\frac{t}{2},t]} \|\tilde{x}_k\|) \quad (20)$$

In case agent f does not follow agent k, the corresponding term γ_{kf} is zero. Similarly, the LFS property of i with respect to $\tilde{x}_1, \ldots, \tilde{x}_L$ is equivalent to:

$$\|\tilde{x}_i(t)\| \leq \beta_i(\|\tilde{x}_i(0)\|, t) + \textstyle\sum_{\ell=1}^{L} \gamma_{\ell i}(\sup \|\tilde{x}_\ell\|) \quad (21)$$

and implies:

$$\sup_{[0,\frac{t}{2}]} \|\tilde{x}_i\| \leq \beta_i(\|\tilde{x}_i(0)\|, 0) + \sum_{\ell=1}^{L} \gamma_{\ell i}(\sup \|\tilde{x}_\ell\|) \quad (22a)$$

$$\sup_{[\frac{t}{2},t]} \|\tilde{x}_i\| \leq \beta_i\left(\left\|\tilde{x}_i(\tfrac{t}{2})\right\|, \tfrac{t}{2}\right) + \sum_{\ell=1}^{L} \gamma_{\ell i}(\sup \|\tilde{x}_\ell\|) \quad (22b)$$

Substituting (19), (22) into (20) yields a new bound:

$$\begin{aligned}\|\tilde{x}_f(t)\| \leq \beta_f\Big(\beta_f\big(\|\tilde{x}_f(0)\|, \tfrac{t}{2}\big) + \sum_{k=1}^{M} \gamma_{kf}\big(\beta_i(\|\tilde{x}_i(0)\|, 0) \\ + \sum_{\ell=1}^{L} \gamma_{\ell i}(\sup \|\tilde{x}_\ell\|)\big), t\Big) + \sum_{\ell=1}^{L} \gamma_{\ell f}\Big(\sup \|\tilde{x}_\ell\|\Big) + \\ \sum_{i=L+1}^{M} \gamma_{if}\Big(\beta_i\big(\beta_i(\|\tilde{x}_i(0)\|, 0) + \sum_{\ell=1}^{L} \gamma_{\ell i}(\sup \|\tilde{x}_\ell\|), \tfrac{t}{2}\big) \\ + \sum_{\ell=1}^{L} \gamma_{\ell i}(\sup \|\tilde{x}_\ell\|)\Big) \quad (23)\end{aligned}$$

Combining (23) with (21) and recalling that for any class-$\mathcal{K}$ function α, $\alpha(x_1 + \cdots + x_n) \leq \alpha(nx_1) + \cdots + \alpha(nx_n)$:

$$\begin{aligned}\|\tilde{x}_f(t)\| \leq \sum_{i=L+1}^{M} \gamma_{if}\Big(2\beta_i\big(2\beta_i(\|\tilde{x}_i(0)\|, 0), \tfrac{t}{2}\big)\Big) + \\ \beta_f\Big(2\beta_f(\|\tilde{x}_f(0)\|, \tfrac{t}{2}) + \sum_{i=L+1}^{M} 2\gamma_{if}\big(2\beta_i(\|\tilde{x}_i(0)\|, 0)\big), t\Big) + \\ \sum_{\ell=1}^{L} \beta_f\Big(2L\big[\sum_{i=L+1}^{M} \gamma_{if}\big(2L\gamma_{\ell i}(\sup \|\tilde{x}_\ell\|)\big) + \gamma_{\ell f}(\sup \|\tilde{x}_\ell\|)\big], 0\Big) \\ + \sum_{\ell=1}^{L} \sum_{i=L+1}^{M} \Big[\gamma_{if}\Big(4L\beta_i\big(2L\gamma_{\ell i}(\sup \|\tilde{x}_\ell\|), 0\big)\Big) \\ + \gamma_{if}\big(4L\gamma_{\ell i}(\sup \|\tilde{x}_\ell\|)\big)\Big] + \sum_{\ell=1}^{L} \gamma_{\ell f}(\sup \|\tilde{x}_\ell\|)\end{aligned}$$

Summing over all $f \in \{M+1,\dots,N\}$ and denoting $\sup\|\tilde{x}_\ell\| \equiv \|\tilde{x}_\ell\|_\infty$ for brevity, we obtain for $\tilde{x} \triangleq (\tilde{x}_{L+1},\dots,\tilde{x}_N)$:

$$\begin{aligned}\|\tilde{x}(t)\| \le & \sum_{i=L+1}^{M} \beta_i(\|\tilde{x}_i(0)\|,t) \\ & + \sum_{f=M+1}^{N}\Big[\sum_{i=L+1}^{M}\gamma_{if}\Big(2\beta_i\big(2\beta_i(\|\tilde{x}_i(0)\|,0),\tfrac{t}{2}\big)\Big)+ \\ & \beta_f\Big(2\beta_f(\|\tilde{x}_f(0)\|,\tfrac{t}{2})+\sum_{i=L+1}^{M}2\gamma_{if}\big(2\beta_i(\|\tilde{x}_i(0)\|,0)\big),t\Big)\Big] \\ & +\sum_{\ell=1}^{L}\sum_{f=M+1}^{N}\gamma_{\ell f}(\|\tilde{x}_\ell\|_\infty)+\sum_{\ell=1}^{L}\sum_{i=L+1}^{M}\sum_{f=M+1}^{N}\Big[\gamma_{if}\big(4L\gamma_{\ell i}(\|\tilde{x}_\ell\|_\infty)\big) \\ & +\gamma_{if}\Big(4L\beta_i\big(2L\gamma_{\ell i}(\|\tilde{x}_\ell\|_\infty),0\big)\Big)\Big]+\sum_{i=L+1}^{M}\gamma_{\ell i}(\|\tilde{x}_\ell\|_\infty)+ \\ & \sum_{\ell=1}^{L}\sum_{f=M+1}^{N}\beta_f\Big(2L\big[\sum_{i=L+1}^{M}\gamma_{if}\big(2L\gamma_{\ell i}(\|\tilde{x}_\ell\|_\infty)\big)+\gamma_{\ell f}(\|\tilde{x}_\ell\|_\infty)\big],0\Big).\end{aligned}$$

Proof of Proposition III.2

The proof follows the same lines as that of Proposition III.1. Note that every follower f is a perturbed system with exponentially stable nominal error dynamics having as a Lyapunov function: $V_f = \tilde{x}_f^T P_f \tilde{x}_f$. This implies that for $\theta \in (0,1)$:

$$\|\tilde{x}_f(t)\| \le \bar{\beta}_f \|\tilde{x}_f(0)\| e^{\frac{-(1-\theta)t}{2\lambda_M[P_f]}} + \sum_{i=L+1}^{M}\bar{\gamma}_{if}\sup\|\tilde{x}_i\|. \quad (24)$$

Expressing (24) for the time intervals $[0,\,\frac{t}{2}]$ and $[\frac{t}{2},t]$ and substituting we obtain:

$$\begin{aligned}\|\tilde{x}_f(t)\| \le & \bar{\beta}_f^2\|\tilde{x}_f(0)\|e^{\frac{-3(1-\theta)t}{4\lambda_M[P_f]}} \\ & +\sum_{i=L+1}^{M}\gamma_{if}\sup_{[\frac{t}{2},t]}\|\tilde{x}_i\|+\bar{\beta}_f e^{\frac{-(1-\theta)t}{2\lambda_M[P_f]}}\sum_{i=L+1}^{M}\bar{\gamma}_{if}\sup_{[0,\frac{t}{2}]}\|\tilde{x}_i\| \\ & +\sum_{\ell=1}^{L}\gamma_{\ell f}\sup_{[\frac{t}{2},t]}\|\tilde{x}_\ell\|+\bar{\beta}_f e^{\frac{-(1-\theta)t}{2\lambda_M[P_f]}}\sum_{\ell=1}^{L}\bar{\gamma}_{\ell f}\sup_{[0,\frac{t}{2}]}\|\tilde{x}_\ell\|. \quad (25)\end{aligned}$$

Similarly, the error for agent i satis£es:

$$\|\tilde{x}_i(t)\| \le \bar{\beta}_i\|\tilde{x}_i(0)\|e^{\frac{-(1-\theta)t}{2\lambda_M[P_i]}}+\frac{2(\lambda_M[P_i])^{\frac{3}{2}}}{(\lambda_m[P_i])^{\frac{1}{2}}\theta}\sup\|\dot{x}_i^r\|.$$

By (1), $\sup\|\dot{x}_i^r\| \le \sum_{\ell=1}^{L}\sup\|\tilde{x}_\ell\|$ which allows us to obtain the bound:

$$\|\tilde{x}_i(t)\| \le \bar{\beta}_i\|\tilde{x}_i(0)\|e^{\frac{-(1-\theta)t}{2\lambda_M[P_i]}}+\textstyle\sum_{\ell=1}^{L}\bar{\gamma}_{\ell i}\sup\|\tilde{x}_\ell\|, \quad (26)$$

Equation (26) now yields the following bounds for the error of an agent i:

$$\sup_{[0,\frac{t}{2}]}\|\tilde{x}_i\| \le \bar{\beta}_i\|\tilde{x}_i(0)\|+\sum_{\ell=1}^{L}\bar{\gamma}_{\ell i}\sup_{[0,\frac{t}{2}]}\|\tilde{x}_\ell\| \quad (27a)$$

$$\sup_{[\frac{t}{2},t]}\|\tilde{x}_i\| \le \bar{\beta}_i\|\tilde{x}_i(\tfrac{t}{2})\|e^{\frac{-(1-\theta)t}{4\lambda_M[P_i]}}+\sum_{\ell=1}^{L}\bar{\gamma}_{\ell i}\sup_{[\frac{t}{2},t]}\|\tilde{x}_\ell\|, \quad (27b)$$

which are then combined with (25) to produce:

$$\begin{aligned}\|\tilde{x}_f(t)\| \le & \bar{\beta}_f^2 e^{\frac{-3(1-\theta)t}{4\lambda_M[P_f]}}\|\tilde{x}_f(0)\|+\sum_{\ell=1}^{L}\bar{\gamma}_{\ell f}\sup\|\tilde{x}_\ell\| \\ & +\sum_{i=L+1}^{M}\bar{\gamma}_{if}\left(\bar{\beta}_i\|\tilde{x}_i(\tfrac{t}{2})\|e^{\frac{-(1-\theta)t}{4\lambda_M[P_i]}}+\sum_{\ell=1}^{L}\bar{\gamma}_{\ell i}\sup_{[\frac{t}{2},t]}\|\tilde{x}_\ell\|\right) \\ & +\bar{\beta}_f e^{\frac{-(1-\theta)t}{2\lambda_M[P_f]}}\sum_{i=L+1}^{M}\bar{\gamma}_{if}\left(\bar{\beta}_i\|\tilde{x}_i(0)\|+\sum_{\ell=1}^{L}\bar{\gamma}_{\ell i}\sup_{[0,\frac{t}{2}]}\|\tilde{x}_\ell\|\right) \\ & +\bar{\beta}_f e^{\frac{-(1-\theta)t}{2\lambda_M[P_f]}}\sum_{\ell=1}^{L}\bar{\gamma}_{\ell f}\sup\|\tilde{x}_\ell\|,\end{aligned}$$

using the fact that for a linear $\mathcal{K}$ class function $\alpha(\cdot)$ it holds $\alpha(x_1,\dots,x_n)=\alpha(x_1)+\cdots+\alpha(x_n)$. Using once again (26) for $\left\|\tilde{x}_i(\frac{t}{2})\right\|$ we £nally arrive at:

$$\begin{aligned}\|\tilde{x}_f(t)\| \le & \bar{\beta}_f^2\|\tilde{x}_f(0)\|e^{\frac{-(1-\theta)t}{2\lambda_M[P_f]}}+ \\ & \sum_{i=L+1}^{M}\big[\bar{\beta}_i\bar{\gamma}_{if}\big(\bar{\beta}_f\|\tilde{x}_i(0)\|e^{\frac{-(1-\theta)t}{4\lambda_M[P_f]}}+\bar{\beta}_i\|\tilde{x}_i(0)\|e^{\frac{-(1-\theta)t}{4\lambda_M[P_i]}}\big) \\ & +\sum_{\ell=1}^{L}\big((1+\bar{\beta}_f)\bar{\gamma}_{\ell f}+(\bar{\beta}_f+\bar{\beta}_i+1)\bar{\gamma}_{if}\bar{\gamma}_{\ell i}\big)\sup\|\tilde{x}_\ell\|\big].\end{aligned}$$

Combining the above with (26) and summing over f:

$$\begin{aligned}\|\tilde{x}(t)\| \le & \sum_{\ell=1}^{L}\sum_{f=M+1}^{N}\Big\{(1+\bar{\beta}_f)\bar{\gamma}_{\ell f}+ \\ & \sum_{i=L+1}^{M}\big((\bar{\beta}_f+\bar{\beta}_i+1)\bar{\gamma}_{if}+1\big)\bar{\gamma}_{\ell i}\Big\}\sup\|\tilde{x}_\ell\| \\ & +\sum_{i=L+1}^{M}\sum_{f=M+1}^{N}(\bar{\beta}_f^2+(\bar{\beta}_i+\bar{\beta}_f)\bar{\beta}_i\bar{\gamma}_{if}+\bar{\beta}_i)\|\tilde{x}(0)\|e^{-\mu t},\end{aligned}$$

where $\mu = \frac{-(1-\theta)t}{2\max\{\lambda_M[P_f],2\lambda_M[P_i]\}}$.

Proof of Proposition IV.1

By de£nition, the LFS gains of the paths of length one are given in matrix form by B_1 and G_1:

$$G_1 = G, \qquad B_1 = B \quad (28a)$$

The gains in paths of length two ending at an agent f can be derived using (9):

$$\begin{aligned}\bar{\gamma}_{\ell f}^{(2)} = & \sum_{i\sim f}\big(\bar{\gamma}_{\ell i}\bar{\gamma}_{if}\bar{\beta}_f+\bar{\gamma}_{\ell i}\bar{\gamma}_{if}+\bar{\gamma}_{\ell i}\bar{\beta}_i\bar{\gamma}_{if}+\bar{\gamma}_{if}\big) \\ & +\bar{\gamma}_{\ell f}(1+\bar{\beta}_f) \quad (29a)\end{aligned}$$

$$\bar{\beta}^{(2)} = \bar{\beta}_f^2+\sum_{k\sim f}\big(\bar{\beta}_k+\bar{\beta}_i^2\bar{\gamma}_{if}+\bar{\beta}_i\bar{\gamma}_{if}\bar{\beta}_f\big). \quad (29b)$$

where $\sim$ denotes vertex adjacency. Equations (29) can be written in matrix form:

$$G_2 = G(G_1 \circ B_1) + GG_1 + (G \circ B)G_1 + GA + G \circ (AB_1 + A^2) \quad (30a)$$

$$B_2 = A(B_1 \circ B_1) + BA + (B \circ B)G_1 + B(G_1 \circ B_1) \quad (30b)$$

where $\circ$ denotes the Schur matrix product (also known as Harramand product) [39]. The Schur product is used to generate the terms $\bar{\gamma}_{ij}\bar{\beta}_j$ and $\bar{\beta}_i^2$ for an arbitrary i. The rightmost term in (29a) is related to the existence of paths of length two between two vertices in Figure 1 which are already connected with an edge. These are identi£ed by the term $G \circ (AB_1)$ as stated in the following Lemma:

Lemma .1. *The elements of the matrix $A \circ A^2$ give the number of paths of length two between any two adjacent vertices.*

Proof. Matrix A^2 has as elements the number of paths of length two between two vertices. On the other hand, the nonzero elements of the adjacency matrix, A, are in positions that correspond to edges in the graph. The Schur product $A \circ A^2$ will therefore have nonzero elements only at positions that correspond to a pair of vertices that are connected both by an edge and by a path of length two. Further, since a nonzero element of $A \circ A^2$ is given by $[a_{ij}] \cdot [a_{ij}]^2 \neq 0$ and the £rst term, $[a_{ij}] = 1$, then necessarily $[a_{ij}] \cdot [a_{ij}]^2 = [a_{ij}]^2 \neq 0$. □

Multiplication by the adjacency matrix of the formation graph, A, shifts the gains of paths of length one from positions at rows $f = M+1, \ldots, N$ to the corresponding positions of their leaders at positions in rows $1, \ldots, M$, based on the fact that powers of the adjacency matrix provide the number of paths between two vertices of length equal to the exponent [35].

Equations (29) and (30) are based on combining the gains of agents $f = M+1, \ldots, N$, that is, $\bar{\beta}_f$, $\bar{\gamma}_{if}$ and $\bar{\gamma}_{\ell f}$, with those of their leaders, $\bar{\beta}_i$ and $\bar{\gamma}_{\ell i}$. The idea now is to apply (30) recursively, starting from the agents at the end of the longest paths and moving towards the formation leaders. In each step, one needs to update the gains of the followers that correspond to positions $f = M+1, \ldots, N$ in the graph of Figure 1, as the latter shifts up towards the formation leaders position. In (30), the gains of agents $1, \ldots, M$ are provided by B and Γ, whereas the gains of $M+1, \ldots, N$ were computed in previous steps.

This is formalized with an induction argument. The induction step is as follows: assume that for some $k < d \leq |\mathcal{V}| - 1$, where d denotes the formation graph diameter, the gains of paths of length $k-1$ are given by matrices B_{k-1} and G_{k-1}. Since all paths of length k ending at an agent i have as a suf£x a path of length $k-1$ ending at i, the former will be represented as paths of length two. Then, by (30), the gain matrices of paths of length k will be:

$$G_k = G(G_{k-1} \circ B_{k-1}) + GG_{k-1} + (G \circ B)G_{k-1} + GA^{k-1} + G \circ (AB_{k-1} + A^k) \quad (31)$$

$$B_k = A(B_{k-1} \circ B_{k-1}) + BA^{k-1} + (B \circ B)G_{k-1} + B(G_{k-1} \circ B_{k-1}). \quad (32)$$

In this way one can compute recursively all paths of length at most $|\mathcal{V}| - 1$.Since this is the maximal path length in any graph with $|\mathcal{V}|$ vertices, the procedure is guaranteed to terminate.

Proof of Proposition V.1

Let the (13) be denoted for brevity as follows:

$$\dot{x} = f(x) + g(x)u \quad (33)$$

where the special "look ahead" structure of $f(x)$ and $g(x)$ is assumed. By de£nition, since the unforced (33) is asymptotically mesh stable, there exists a class-$\mathcal{KL}$ function $\beta(r,t)$ such that:

$$\|x\| \leq \beta(\|x(0)\|, t), \quad \forall t \geq 0.$$

A converse Lyapunov argument for the unforced (33) establishes the existence of a Lyapunov function $V(x)$, such that for some class-$\mathcal{K}$ functions $\alpha_1(\cdot)$, $\alpha_2(\cdot)$, $\alpha_3(\cdot)$, $\alpha_4(\cdot)$, it holds:

$$\alpha_1(\|x\|) \leq V(x) \leq \alpha_2(\|x\|)$$
$$\frac{\partial V}{\partial t} + \frac{\partial V}{\partial x} f(x) \leq -\alpha_3(\|x\|), \qquad \left\| \frac{\partial V}{\partial x} \right\| \leq \alpha_4(\|x\|)$$

Then for (33) with $u \neq 0$, the Lyapunov function V will satisfy:

$$\alpha_1(\|x\|) \leq V(x) \leq \alpha_2(\|x\|), \quad \left\| \frac{\partial V}{\partial x} \right\| \leq \alpha_4(\|x\|)$$
$$\frac{\partial V}{\partial t} + \frac{\partial V}{\partial x}(f(x) + g(x)u) \leq -\alpha_3(\|x\|) + \zeta(\|x\|)\alpha_4(\|x\|)\,\|u\|$$

From stability of perturbed system it follows that

$$\|x(t)\| \leq \beta(\|x\|(0), t) + \alpha_1^{-1}(\alpha_2(\alpha_3^{-1}(\kappa \sup \|u\|)))$$

where $\kappa = \frac{\zeta(r)\alpha_4(r)}{\theta}$, $\theta \in (0,1)$.